The Role of Substrate Identity in Determining Monolayer Motional Relaxation Dynamics

J. C. Horne and G. J. Blanchard*,[1]

Contribution from the Michigan State University, Department of Chemistry, East Lansing, Michigan 48824-1322

Received July 28, 1997

Abstract: We report on the lifetime and motional dynamics of Zirconium Phosphonate (ZP) monolayers containing oligothiophene chromophores in a range of concentrations. Monolayers were formed on fused silica substrates and on a 15 Å oxide layer formed on crystalline Si(100) substrates. For both interfaces, the fluorescence lifetime behavior of the chromophores is identical and does not depend on chromophore concentration within the monolayer. Transient anisotropy measurements reveal that, for both substrates, the chromophores are oriented at ∼35° with respect to the surface normal. For monolayers formed on silica, there is no evidence for chromophore motion, while motion is seen for monolayers formed on silicon. Despite the substantial similarity between the two families of monolayers, the surface roughness of the primed silicon substrate allows for greater motional freedom of the chromophores in the monolayers. We discuss these findings in the context of the differences in substrate surface roughness and domain sizes as measured by atomic force microscopy (AFM).

Introduction

Interfacial molecular assemblies have achieved wide use for the modification of surfaces. Surface-modified materials have potential application in many areas including tribology, nonlinear optics, and device patterning.[2−9] The most widely examined self-assembled monolayers (SAMs) are formed from alkanethiols on gold.[10,11] While this family of monolayers has been investigated extensively, the opportunity to form complex interfacial structures is limited unless specially functionalized molecules are used in the formation of the initial layer.[12−17] For alkanethiol monolayers, the terminal methyl groups effectively preclude chemical addition beyond the first layer, and alternative chemistries that allow for the facile formation of multiple layers have been developed to circumvent this problem. Metal-phosphonate (MP) chemistry has proven to be a remarkably effective and robust route to the formation of multilayer assemblies.[18−34] Like other systems that exhibit mesoscopic organization, metal phosphonate structures have been used successfully in many studies, including optical second harmonic generation, artificial photosynthesis, and light harvesting.[7,28,29,35−37]

Layered metal phosphonates are attractive materials for several reasons. Synthesis of the layered assemblies is simple, involving immersion of a primed substrate into alternating metal ion and α,ω-bisphosphonate solutions. The low solubility of the complex formed between phosphonates and several metal ions makes the structures especially robust, in contrast to Langmuir−Blodgett layers, which are characterized by weak interlayer associations. Zirconium phosphonate (ZP) layered

(1) To whom correspondence should be addressed.

(2) Bain, C. D.; Whitesides, G. M. *Science* **1988**, *240*, 62.
(3) Wilbur, J. L.; Biebuyck, H. A.; MacDonald, J. C.; Whitesides, G. M. *Langmuir* **1995**, *11*, 825.
(4) Drawhorn, R. A.; Abbott, N. L. *J. Phys. Chem.* **1995**, *99*, 16511.
(5) Xia, Y.; Zhao, X.-M.; Kim, E.; Whitesides, G. M. *Chem. Mater.* **1995**, *7*, 2332.
(6) Ford, J. F.; Vickers, T. M.; Mann, C. K.; Schlenoff, J. B. *Langmuir* **1992**, *12*, 1944.
(7) Kim, E.; Whitesides, G. M.; Lee, L. K.; Smith, S. P.; Prentiss, M. *Adv. Mater.* **1996**, *8*, 139.
(8) Katz, H. E.; Wilson, W. L.; Scheller, G. *J. Am. Chem. Soc.* **1994**, *116*, 6636.
(9) Neff, G. A.; Zeppenfeld, A. C.; Klopfenstein, B.; Page, C. J. *Mater. Res. Soc. Symp. Proc.* **1994**, *351*, 269.
(10) Dubois, L. H.; Nuzzo, R. G. *Annu. Rev. Phys. Chem.* **1992**, *43*, 437.
(11) Ulman, A. *Chem. Rev.* **1996**, *96*, 1533.
(12) Nuzzo, R. G.; Dubois, L. H.; Allara, D. L. *J. Am. Chem. Soc.* **1990**, *112*, 558.
(13) Whitesides, G. M.; Laibinis, P. E. *Langmuir* **1990**, *6*, 87.
(14) Frey, B. L.; Hanken, D. G.; Corn, R. M. *Langmuir* **1993**, *9*, 1815.
(15) Sun, L.; Kepley, L. J.; Crooks, R. M. *Langmuir* **1992**, *8*, 2101.
(16) Kepley, L. J.; Crooks, R. M.; Ricco, A. J. *Anal. Chem.* **1992**, *64*, 3191.
(17) Green, J.-B. D.; McDermott, M. T.; Porter, M. D. *J. Phys. Chem.* **1996**, *100*, 13342.
(18) Hong, H.-G.; Sackett, D. D.; Mallouk, T. E. *Chem. Mater.* **1991**, *3*, 521.
(19) Thompson, M. E. *Chem. Mater.* **1994**, *6*, 1168.
(20) Katz, H. E.; Wilson, W. L.; Scheller, G. *J. Am. Chem. Soc.* **1994**, *116*, 6636.
(21) Yonemoto, E. H.; Saupe, G. B.; Schmehl, R. H.; Hubig, S. M.; Riley, R. L.; Iverson, B. L.; Mallouk, T. E. *J. Am. Chem. Soc.* **1994**, *116*, 4786.
(22) Katz, H. E.; Bent, S. F.; Wilson, W. L.; Schilling, M. L.; Ungashe, S. B. *J. Am. Chem. Soc.* **1994**, *116*, 6631.
(23) Frey, B. L.; Hanken, D. G.; Corn, R. M. *Langmuir* **1993**, *9*, 1815.
(24) Yang, H. C.; Aoki, K.; Hong, H.-G.; Sackett, D. D.; Arendt, M. F.; Yau, S.-L.; Bell, C. M.; Mallouk, T. E. *J. Am. Chem. Soc.* **1993**, *115*, 11855.
(25) Vermeulen, L.; Thompson, M. E. *Nature* **1992**, *358*, 656.
(26) Ungashe, S. B.; Wilson, W. L.; Katz, H. E.; Scheller, G. R.; Putvinski, T. M. *J. Am. Chem. Soc.* **1992**, *114*, 8717.
(27) Cao, G.; Rabenberg, L. K.; Nunn, C. M.; Mallouk, T. E. *Chem. Mater.* **1991**, *3*, 149.
(28) Katz, H. E.; Schilling, M. L.; Chidsey, C. E. D.; Putvinski, T. M.; Hutton, R. S. *Chem. Mater.* **1991**, *3*, 699.
(29) Katz, H. E.; Scheller, G.; Putvinski, T. M.; Schilling, M. L.; Wilson, W. L.; Chidsey, C. E. D. *Science* **1991**, *254*, 1485.
(30) Putvinski, T. M.; Schilling, M. L.; Katz, H. E.; Chidsey, C. E. D.; Mujsce, A. M.; Emerson, A. B. *Langmuir* **1990**, *6*, 1567.
(31) Rong, D.; Hong, H.-G.; Kim, Y.-I.; Krueger, J. S.; Mayer, J. E.; Mallouk, T. E. *Coord. Chem. Rev.* **1990**, *97*, 237.
(32) Lee, H.; Kepley, L. J.; Hong, H.-G.; Akhter, S.; Mallouk, T. E. *J. Phys. Chem.* **1988**, *92*, 2597.

S0002-7863(97)02574-2 CCC: $15.00
Published on Web 06/05/1998

Scheme 1. Structures of Oligobisphosphonates Used in This Work: (a) 2,2′-Bithiophene-5,5′-diylbis(phosphonic acid) (BDP); (b) 2,2′:5′,2″:5″,2‴-Quaterthiophene-5,5‴-diylbis-(phosphonic acid) (QDP); (c) 1,12-Dodecanediylbis-(phosphonic acid) (DDBPA); (d) 1,6-Hexanediylbis-(phosphonic acid) (HBPA)

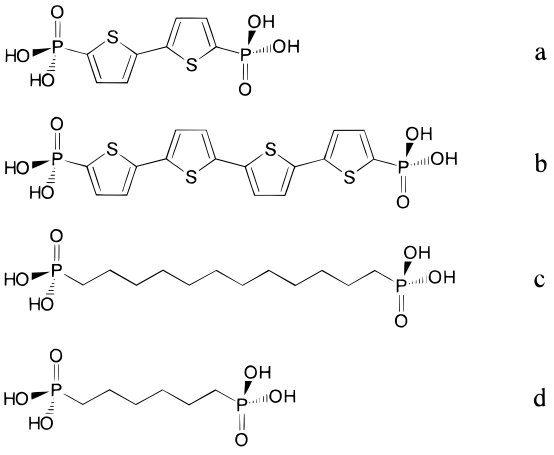

complexes are most common, but other metal ions have been used as well.[23,38,39] The structures are built up one layer at a time with control over the specific molecular identity of each layer, affording exquisite control over the chemical, electrical, or optical properties of each layer and, consequently, of the entire film.

One application for which three-dimensional, layer-by-layer control of multilayer structure could potentially be useful is in optical information storage. Present-day storage devices use a single layer medium, and the addition of a useful third dimension could enhance the storage density of a given volume of the surface. The use of MP multilayers with chemically and optically distinct layers could be the foundation for such a three-dimensional structure, but there are aspects of this scheme that could serve to limit the utility of these materials for information storage. The lateral dimensions of each physical resolution unit in a MP assembly will be determined by the diffraction limit of the optical system used to read and write the information. The stability and layer-specificity of the information written to the material is key to the implementation of such an approach. The chemical change associated with writing or erasing, while still under investigation, will likely be a cis−trans isomerization but, in any event, will involve the excited electronic state of the molecule. The conformational change must be an activated process with a sufficiently high barrier to ensure that the operation is irreversible under ambient dark conditions. The layer constituents must also be resistant to oxidative- or photodegradation over long periods of time and use, and there is the possibility of excitation transport from one region of the assembly to another, within a single layer or between constituents in neighboring layers.

The purpose of this work is not to identify candidate molecules for the actual storage of information but rather to consider the fundamental issue that, regardless of the chemical structure of the information-carrying molecule, any change in logic state will be mediated by the excited state of the molecule. It is therefore important to place fundamental limits on the physical and chemical consequences of effecting an optical excitation in a multilayer assembly. Our focus is to understand the energy migration and motional dynamics that occur within an optically active layer. By using simple chromophores, we can observe the presence or absence of excitation transport and motional dynamics without complications associated with large scale chromophore isomerization. We use oligothiophenes as chromophores because they are relatively well understood and form ordered layers due to their rigid structure. We chose 2,2′-bithiophene-5,5′-diylbis-(phosphonic acid) (BDP) and 2,2′:5′,2″:5″,2‴-quaterthiophene-5,5‴-diylbis(phosphonic acid) (QDP) (Scheme 1) because the BDP emission band overlaps the QDP absorption band, as shown in Figure 1. The spectral overlap of the two chromophores is useful for excitation transport studies. These chromophores can photoisomerize via ring rotation[40] and this property is of value in understanding their dynamical response in layered assemblies (*vide infra*).

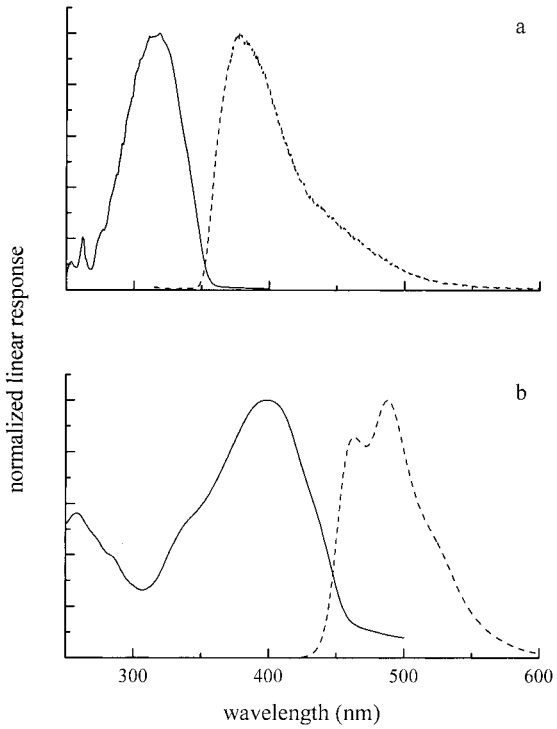

Figure 1. Absorption (—) and emission (− − −) spectra for (a) BDP and (b) QDP solutions (10^{-5} M) in DMSO.

In these initial studies, we concentrate on the intralayer motional relaxation properties of each chromophore by varying the chromophore concentration in a series of BDP and QDP monolayers. The chromophore concentration is controlled by incorporating optically inactive, alkanebisphosphonate diluents into the monolayer. We chose 1,6-hexanediylbis(phosphonic acid) and 1,12-dodecanediylbis(phosphonic acid) as diluents because, in their all-trans conformations, they are approximately the same lengths as BDP and QDP, respectively, enabling us to make the monolayer thickness as uniform as possible, at least on molecular length scales.

We have characterized the chromophore dynamics of a single layer of BDP on fused silica substrates previously.[41] In this work, we compare the behavior of QDP to BDP on fused silica and oxidized Si(100) substrates. For BDP on silica, we do not detect any chromophore rotational motion. The fluorescence

(33) Lee, H.; Kepley, L. J.; Hong, H.-G.; Mallouk, T. E. *J. Am. Chem. Soc.* **1988**, *110*, 618.
(34) Katz, H. E. *Chem. Mater.* **1994**, *6*, 2227.
(35) Vermeulen, L. A.; Snover, J. L.; Sapochak, L. S.; Thompson, M. E. *J. Am. Chem. Soc.* **1993**, *115*, 11767.
(36) Snover, J. L.; Byrd, H.; Suponeva, E. P.; Vicenzi, E.; Thompson, M. E. *Chem. Mater.* **1996**, *8*, 1490.
(37) Kaschak, D. M.; Mallouk, T. E. *J. Am. Chem. Soc.* **1996**, *118*, 4222.
(38) Neff, G. A.; Mahon, T. M.; Abshere, T. A.; Page, C. J. *Mater. Res. Symp. Proc.* **1996**, *435*, 661.
(39) Feldheim, D. L.; Mallouk, T. E. *Chem. Commun.* **1996**, 2591.

Scheme 2. Conformations of QDP with Thiophene Rings (a) All Anti and (b) All Syn and Conformations of BDP with Thiophene Rings (c) Anti and (d) Syn

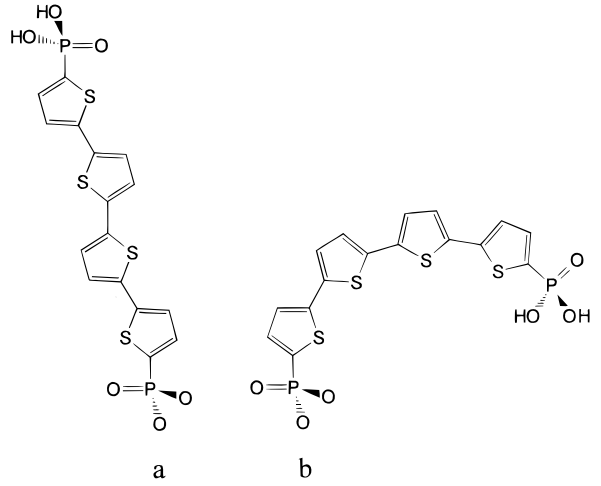

dynamics of QDP on silica are essentially the same, as we describe below in more detail.

The identity of the substrate affects the dynamical behavior of the chromophores. The 15 Å oxide layer on Si(100) possesses the same active sites (−OH) as silica, but there are fundamental differences in site density and surface roughness on oxidized silicon that affect the primer density and organization and thus influence the adlayers. The steady-state optical response and the fluorescence lifetime behavior were identical on both substrates, for a given chromophore. We detect chromophore motion on silicon, and this finding suggests substantially different organization and structural freedom in the two systems. The active sites on silica appear to allow a higher chromophore density on the initial phosphonate primer layer than is seen for silicon, giving rise to an improvement in the ordering of the first layers. We present AFM images of the SiO_x substrates that complement the dynamic spectroscopic measurements and demonstrate the differences in surface roughness of the substrates.

Experimental Section

Synthesis of 2,2′:5′,2″:5″,2‴-Quaterthiophene-5,5‴-diylbis(phosphonic acid) (QDP) and 2,2′-Bithiophene-5,5′diylbis(phosphonic acid) (BDP). QDP was synthesized with minimal modification of a procedure published previously.[27] Tetrahydrofuran (THF) was distilled over CaH_2 and sodium before use. Quaterthiophene (QT) was prepared by the reaction of 20 mmol bithiophene (Aldrich Chemical Co.) in THF with 1 equiv of *n*-butyllithium (2.5M in hexanes, Aldrich) at −78 °C for 20 min. The mixture was transferred by cannula to a second flask containing a suspension of anhydrous $CuCl_2$ (excess) in THF. The clear yellow solution was allowed to warm slowly to room temperature and was stirred overnight. The addition of 50 mL of 1 M HCl resulted in the formation of a yellow precipitate in a brown-green solution, which was vacuum filtered and dried (64% yield). A solution of QT (3 mmol) in THF was cooled to −40 °C, and an excess (12.5 mmol) of *n*-BuLi was added. After stirring for 2 h, a second solution of 12.5 mmol bis(dimethylamino)phosphochloridate (Aldrich) and 0.625 mmol *n*-BuLi in THF was added to the first solution via cannula, and the resulting solution was allowed to warm to room temperature. The reaction was stopped after 3 days, the product was extracted from water with ether, and the aqueous layer was extracted twice with CH_2Cl_2. The product was purified chromatograpically on silica plates (Fisher) using a mobile phase of 1:1 CH_2Cl_2 and THF. The most polar component was collected in 46% yield. A portion of this tetraamide was dissolved in dioxane at 80 °C. The solution was acidified with 50 mL each of H_2O and concentrated HCl and refluxed overnight. Upon cooling to room temperature, bright yellow QDP precipitated from solution and was collected by vacuum filtration in 55% yield. Overall yield was 21%. ^{1}H NMR (DMSO-d_6): 7.4 ppm (m). The phosphorylation of bithiophene to synthesize 2,2′-bithiophene-5,5′-diylbis-(phosphonic acid) (BDP) was very similar and has been reported elsewhere.[40]

Synthesis of 1,12-Dodecanediylbis(phosphonic acid) (DDBPA) and 1,6-Hexanediylbis(phosphonic acid) (HBPA). All chemicals used in the synthesis were purchased from Aldrich Chemical Co. Triethyl phosphite was treated with sodium and vacuum distilled. DDBPA was prepared by the Michaelis-Arbuzov reaction[42] of 1,12-dibromododecane with triethyl phosphite. The mixture was refluxed for 5 h to allow evolution of ethyl bromide. Excess triethyl phosphite was removed by vacuum distillation. Concentrated HCl was added to the solution, which was then refluxed for 12 h, and the resulting white precipitate was collected by vacuum filtration and washed with acetonitrile. The yield was 68%. ^{1}H NMR (DMSO-d_6): 1.2−1.5 ppm (m). The synthesis of HBPA was identical, using 1,6-dibromohexane as starting material.

Metal-Phosphonate Multilayer Synthesis. Fused silica and polished Si(100) (MultiScanning Plus) substrates were cleaned by piranha solution etch *(Caution! Piranha solution is extremely corrosive and is a potent oxidizer)* for 10 min and rinsed with flowing distilled water, followed by hydrolysis in 2 M HCl for 5 min, and a final distilled water rinse. Samples were dried with a N_2 stream and used shortly after for deposition. The substrates were primed by reflux in a 1% v/v solution of 3-(aminopropyl)triethoxysilane in anhydrous octane for 10 min, followed by rinses with hexane and water. After drying with N_2, the amine surface was derivatized to the phosphonate in a solution of 0.1 M $POCl_3$ and 0.1 M collidine in anhydrous CH_3CN for 1 h, followed by rinses with CH_3CN and water. The resulting surface was functionalized with Zr^{4+} by immersion in a 5 mM solution of $ZrOCl_2$ in 60% aqueous ethanol solution for 10 min. Monolayers were deposited from bisphosphonate solutions with a total 1 mM concentration ([chromophore] + [alkane] = 1 mM). Alkanebisphosphonate, BDP, and mixed alkanebisphosphonate/BDP solutions were made in 90% EtOH (aq); QDP and mixed alkanebisphosphonate/QDP were made in 80% DMSO, 20% (90% EtOH (aq)). The substrates were immersed in the appropriate bisphosphonate solution for 4 h at 55 °C.

Steady-State Optical Spectroscopy. The absorbance spectra of oligothiophene chromophores in solution and on surfaces were measured using a Hitachi U-4001 UV−visible spectrophotometer. Monolayer samples were held vertically in place at a 45° angle with respect to the incident beam. Spectra were collected with 5 nm resolution. Fluorescence spectra of solutions were measured on a Hitachi F-4500 fluorescence spectrophotometer. Excitation and emission slits were adjusted according to spectral intensity. Monolayer emission spectra were collected on a SPEX Fluorolog 2 spectrophotometer. Samples were mounted vertically and at a 45° angle with respect to excitation, to minimize reflection of excitation light into the emission collection optics. Slits were adjusted according to spectral intensity.

Time Correlated Single Photon Counting Spectroscopy (TCSPC). TCSPC was used to measure excited-state fluorescence lifetimes and rotational dynamics of the chromophores. This system has been described in detail previously,[43] and we review it briefly here. The light pulses used to excite the sample are generated with a cavity dumped, synchronously pumped dye laser (Coherent 702−2) pumped by the second harmonic output of a mode-locked CW Nd:YAG laser (Quantronix 416). The excitation beam was frequency doubled ($LiIO_3$ Type I SHG) to excite BDP samples at 320 nm (640 nm fundamental, Kiton Red, Exciton) and QDP samples at 390 nm (780 nm fundamental, LDS 821, Exciton). Monolayer samples were held approximately horizontally, with 5° tilts away from the horizontal in two directions: toward the excitation beam and toward the detector. Fluorescence from the sample was imaged through a reflecting microscope objective. Lifetimes were collected across the emission bands at 54.7° with respect to the excitation polarization for solutions and without polarization bias for monolayers. While such collection can, in principle, lead to small contributions to the measured relaxation from motional dynamics, for

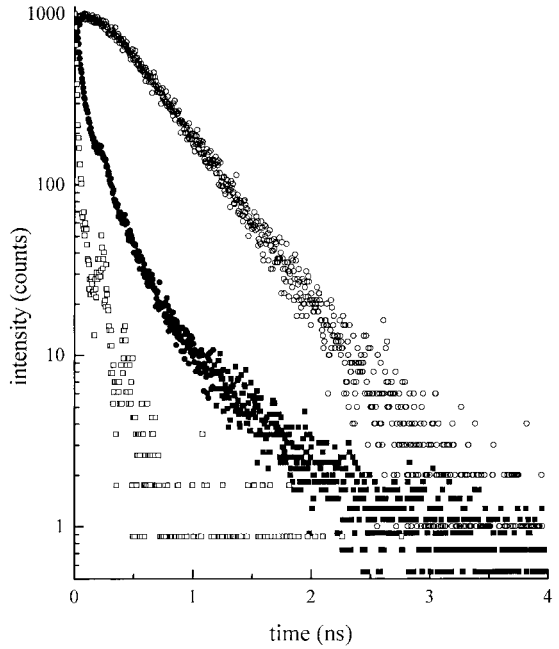

Figure 2. Representative instrument response function (□), excited-state population decay for QDP in DMSO (10^{-5} M) (○) and excited-state population decay for QDP in a monolayer (1%) (●).

our experimental conditions this is not a problem.[44,45] Fluorescence was collected at 390 and 465 nm (5 nm fwhm bandwidth for solution, 30 nm for monolayers) for BDP and QDP, respectively, with polarizations of 0° and 90° for orientational anisotropy measurements on all samples. A representative lifetime decay and instrument response function (~35 ps fwhm) are shown in Figure 2.

Data Analysis. The lifetimes we report here were fit to sums of exponentials using commercial software (Microcal Origin) and are reported as the averages and standard deviations of 4−6 individual decays. Rotational dynamics parameters were determined in two ways. For monolayers on silica, eight pairs of alternating parallel and perpendicular scans were used to produce an average anisotropy function. Each scan pair was recorded for a different physical location on the substrate. $R(0)$ was determined to ±0.01 by regression of data at times after the instrumental response, and several data sets were averaged for each sample. For monolayers on oxidized Si(100), the rotational diffusion information is reported as the averages and standard deviations of data from several decays. Four pairs of alternating parallel and perpendicular scans were used to produce an average anisotropy function, which was fit with Origin to determine the parameters $R(0)$, τ_{MR}, and $R(\infty)$.

Calculations. Semiempirical calculations were performed using Hyperchem Release 4.0 (Hypercube, Inc.). The PM3 parametrization used for these calculations is a modification of the AM1 parametrization that treats molecules containing heteroatoms, such as sulfur, more accurately than previous parametrizations. An initial optimization of the structure was performed using a molecular mechanics routine (MM+) followed by geometry optimization at the semiempirical level using an SCF algorithm. The torsions of the QDP 2-2′ and 5′-5″ σ bonds were set at 10° increments, and semiempirical optimization was performed until the lowest energy conformation for the fixed interring bond torsions was reached. The heat of formation and $S_0 \leftrightarrow S_1$ transition energy were calculated for each geometrically optimized conformation.

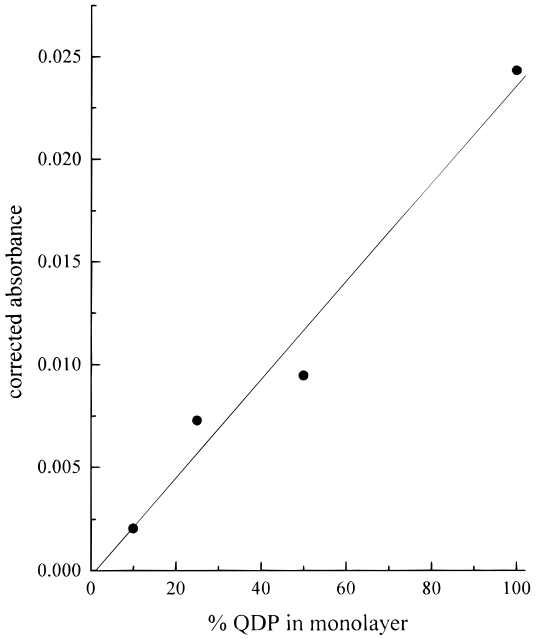

Figure 3. Dependence of monolayer absorbance on concentration of QDP in deposition solution and regression of experimental data.

Results and Discussion

In this section we compare the steady-state and transient optical responses of four optically active chemical systems using two chromophores and two substrates. A basic understanding of the optical response and the intralayer relaxation effects of each chromophore is necessary for future investigation of interlayer energy transport between the two chromophores in complex multilayer structures. In addition to the determination of the optical properties of these layers, the effect of substrate must also be considered. Several measurements contribute to our understanding of the optical response, including UV−visible absorption, fluorescence emission, excited-state population decays, and induced orientational anisotropy. The results from the anisotropy measurements are critical for comparing the systems. We detail the subtle differences between the systems below.

Monolayers on Fused Silica. Steady-State Spectroscopy. BDP monolayers on silica were characterized previously.[40] For BDP and HBPA mixed monolayers, we found a linear relationship between the proportion of chromophore in the deposition solution and the proportion of chromophore in the resulting monolayer. The calibration did not regress through the origin, however. This is a simple partitioning effect and can be understood in terms of preferential solvation of HBPA over BDP in ethanol. For QDP and DDBPA mixed monolayers, we also observe a calibration that is linear in QDP concentration, shown in Figure 3. In this case, the solvent system used for the monolayer deposition solution gives rise to a calibration curve that passes through the origin. The implication of these data is that solution concentration ratios will result in a monolayer with the same constituent ratio, if the solvent system is chosen correctly. The proportions of constituents that are incorporated into a mixed monolayer depend mostly on their solubilities in the solvent used.

The steady-state emission spectra for both BDP and QDP are similar in the sense that they reveal more than one form of the chromophore in the monolayer. The BDP spectrum has two features, a narrow peak at 390 nm that we see for dilute (<35% BDP) monolayers and a broader, less intense peak at 425 nm

(40) Horne, J. C.; Blanchard, G. J.; LeGoff, E. *J. Am. Chem. Soc.* **1995**, *117*, 9551.
(41) Horne, J. C.; Blanchard, G. J. *J. Am. Chem. Soc.* **1996**, *118*, 12788.
(42) Bhattacharya, A. K.; Thyagarajan, G. *Chem. Rev.* **1981**, *81*, 415.
(43) DeWitt, L.; Blanchard, G. J.; LeGoff, E.; Benz, M. E.; Liao, J. H.; Kanatzidis, M. G. *J. Am. Chem. Soc.* **1993**, *115*, 12158.
(44) Flory, W. C.; Blanchard, G. J. *Appl. Spectrosc.* **1998**, *52*, 82.
(45) Spencer, R. D.; Weber, G.; *J. Chem. Phys.* **1970**, *52*, 1654.

Table 1. Excited State Lifetimes of Monolayers[a]

	τ_1 (ps)	τ_2 (ps)
BDP on silica	187 ± 11	1140 ± 337
QDP on silica	232 ± 16	1265 ± 138
BDP on silicon	213 ± 12	1277 ± 96
QDP on silicon	243 ± 23	1115 ± 156

[a] The time constants refer to fits of the experimental data to the function $f(t) = A_1 \exp(-t/\tau_1) + A_2 \exp(-t/\tau_2)$.

that we observe for concentrated monolayers. These bands correspond to the two peaks present in concentrated solution spectra. QDP exhibits four unresolved bands in solution and typically three are present in monolayer spectra (see Figure 4a,b). For the monolayers, the 445 nm band is not observed. The QDP spectra also depend on concentration in the monolayer. Blue-shifted peaks are prominent in the dilute monolayer spectra, and red-shifted features dominate the concentrated monolayer spectra. Over time, the BDP spectra anneal to spectrum dominated by the blue band,[40] but it is not clear from our data that QDP monolayers exhibit this same evolution. The complexity of these monolayer spectra is also manifested in the temporal evolution of emission intensity. We will discuss this behavior in more detail in a forthcoming paper.[46]

Transient Spectroscopies. The dilute solution behavior of both BDP and QDP is that of a simple chromophore. The absorption and emission bands of the steady-state spectra are well-defined, and dilute solution lifetimes are fit to a single exponential decay for both chromophores. The lifetime for dilute solutions is approximately 200 ps for BDP and 450 ps for QDP. The population decays of monolayers approximate a double exponential, as shown in Figure 2. The fast component of the monolayer lifetimes is ∼ 200 ps for both chromophores and the longer lifetime is ∼ 1.2 ns, as shown in Table 1. We interpret the fast monolayer lifetime as that due primarily to an isolated chromophore species in an alkane-like environment, owing to its similarity to the solution phase value, and the long lifetime primarily to a chromophore within an aggregated island. These assignments are, of course, only approximations, and the actual contributions to the measured decay are not as clear-cut. This relaxation behavior is well understood, and we will present a detailed treatment elsewhere.[45] The lifetimes do not vary with respect to either chromophore density in the monolayer or emission wavelength collected for either chromophore. For this reason, the lifetimes reported in Table 1 are averages over all concentrations and emission wavelengths used for chromophore monolayers. However, the fractional contribution of each lifetime component varies with chromophore concentration and emission wavelength. For BDP, as the chromophore concentration is increased or as emission is collected on the red edge of the emission band, the relative contribution of the long lifetime increases. This trend is not observed with QDP, as the contributions of the different species to the total signal varied with no simple pattern. This effect may be due to the greater complexity of the QDP emission spectrum compared to BDP.

Rotational motion measurements are not complicated by population decay functionality effects and can provide insight into how the chromophores move within their environment, offering an indication of how ordered the layers are. Rotational diffusion measurements are most typically made on probe molecules in solution, where the chromophores can relax into all possible orientations. We have measured the dynamics of BDP and QDP in monolayers. Because one end of each chromophore is attached to a substrate, the motion of the chromophore is confined to a conic volume. The cone dimensions are described by Lipari and Szabo's hindered rotor

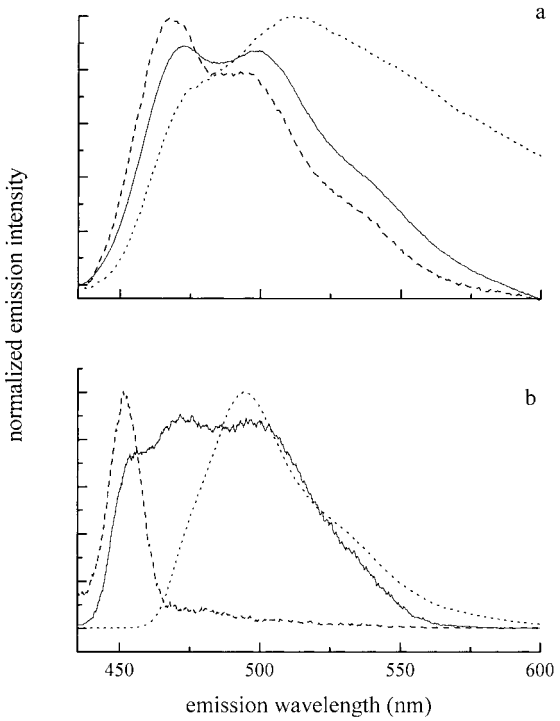

Figure 4. Emission spectra of (a) QDP monolayers (− − −) 1%; (—) 5%; (•••) 100% and (b) QDP solution in DMSO (− − −) 10^{-7} M; (—) 10^{-6} M; (•••) 10^{-3} M. Spectra were normalized for presentation, and no information about fluorescence quantum yield should be inferred from these plots.

model,[47] where the base of the cone is the point of attachment of the chromophore to the substrate, and the semiangle of the cone is designated θ_0. A nonrandom orientational distribution of the chromophore ensemble in the monolayer is selected with a polarized excitation pulse, and components of the emission that are polarized parallel and perpendicular to the excitation polarization are collected. These data (Figure 5a, for example) are combined to construct the induced orientational anisotropy function, $R(t)$

$$R(t) = \frac{I_{\parallel}(t) - I_{\perp}(t)}{I_{\parallel}(t) + 2I_{\perp}(t)} \tag{1}$$

The decay of $R(t)$ (see Figure 5b) is fit to

$$R(t) = R(\infty) + [R(0) - R(\infty)] \exp(-t/\tau_{MR}) \tag{2}$$

τ_{MR} is the motional relaxation time constant and the quantity $R(0)$ is related to the angle between the chromophore absorbing and emitting transition moments, δ

$$R(0) = \frac{2}{5} P_2(\cos \delta) \tag{3}$$

where P_2 is the second-order Legendre polynomial. For BDP in solution, $R(0) = 0.24$, which corresponds to an angle of $\delta = 31°$. For QDP in solution, $R(0) = 0.40$, indicating parallel transition moments. We consider that the QDP transition moments lie along the long molecular axis. We use these values for δ in the treatment of monolayer data because this quantity is intrinsic to the chromophore and, for the solution data, represents an average over all conformers. We note that $R(0)$ does depend to a certain extent on environment because the intramolecular rotational freedom available to the chromophore depends on the limitations imposed by its surroundings (*vide*

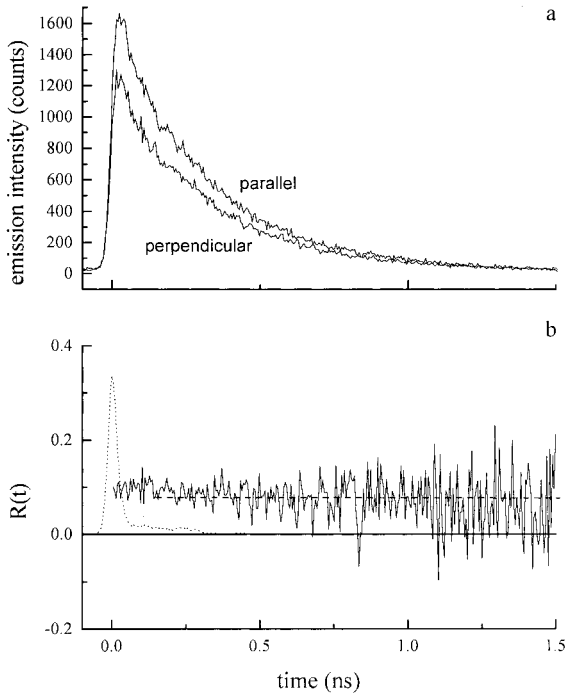

Figure 5. Reorientation data for a 50% QDP monolayer on silica. (a) Emission intensity data for parallel and perpendicular polarizations. (b) Induced orientational anisotropy function of above data with fit (− − −).

Table 2. Induced Orientational Anisotropy Data for Monolayers[a]

	$R(0)$	τ_{MR} (ps)	$R(\infty)$	θ (deg)
BDP on silica			0.06 ± 0.01	35 ± 2
QDP on silica			0.07 ± 0.05	39 ± 7
BDP on silicon	0.40 ± 0.15	393 ± 119	0.18 ± 0.08	19 ± 11
QDP on silicon	0.32 ± 0.06	479 ± 153	0.13 ± 0.06	32 ± 7

[a] For BDP, the angle between the transition moments is $\delta = 31°$ and for QDP, $\delta = 0°$. Angles θ were determined from δ and $R(\infty)$ data using eq 4.

infra). Specifically, syn and anti conformers are likely to exhibit different values of δ.

For chromophores in solution, $R(\infty) = 0$ because they can completely re-randomize at infinite time. For chromophores in monolayers, $|R(\infty)| > 0$ because of the geometric restriction on their motional freedom. $R(\infty)$, the steady-state anisotropy, is related to θ, the average tilt angle of the chromophore within the cone by[46]

$$R(\infty) = \frac{2}{5}P_2(\cos\theta_{ex})P_2(\cos\theta_{em})\langle P_2(\cos\theta)\rangle^2 \qquad (4)$$

The angles θ_{ex} and θ_{em} are the transition moment angles with respect to the cone center axis. The calculation of θ is simplified by setting $\theta_{ex} = 0°$ and $\theta_{em} = \delta$. In our previous work we reported that BDP on SiO_x exhibited a concentration-independent steady-state anisotropy of 0.06 ± 0.01, which yields an average tilt angle of $35° \pm 2°$.[40] We report here that QDP on silica has a similar, concentration-independent steady-state anisotropy of 0.07 ± 0.05 and an average tilt angle of $39° \pm 7°$ (Table 2). Our measurement of the same tilt angles for both chromophores implies that the oligothiophene/alkane environment is not affected by the lengths of the constituent molecules. We note that the angles we report here for layer tilt are quite similar to the tilt angle of ~30° seen for alkanethiol monolayers on gold.[9] In the case of alkanethiol/gold SAMs, the tilt angle is determined by aliphatic interchain interactions and the registry of the thiol headgroups on the crystalline gold substrate surface. For ZP layers, it is not as obvious that intermolecular interactions dominate the tilt angle because, for the substrates we use, the spacing between primed sites is significantly less well determined than for a crystalline metal surface. In the case of ZP layers, it may be the bonding geometry of the metal-phosphonate connecting layers that determines the range of structural properties available to the system.

We do not detect any chromophore motion in either BDP or QDP monolayers on silica, as indicated by the absence of a decay in $R(t)$.[40,48] At times after the instrument response function, regression of $R(t)$ yields a line of zero slope. We can evaluate the possibility that the chromophores are reorienting significantly faster than our detection system time resolution (~35 ps). The time constants of reorientation in solution are 299 ± 15 ps for BDP in ethanol and 1.2 ± 0.2 ns for QDP in DMSO. Based on viscosity considerations, we believe that the chromophore imbedded in the monolayer will not reorient more rapidly than in low viscosity solvents such as ethanol or DMSO. If there was any motion of the chromophore in the monolayer, it would occur on a time scale we can determine because of the proximity of neighboring molecules and dipolar and van der Waals interactions between them.

Monolayers on Silicon. The substrate on which self-assembling structures are synthesized affects the ordering of the adlayers.[9,10,49−53] This effect is seen for alkanethiol layers on various metal surfaces, because the infrared-active symmetric and asymmetric CH_2 stretching modes are sensitive indicators of aliphatic chain ordering. We compare the optical response of the chromophore monolayers on silica to that on oxidized Si(100) substrates to evaluate the role of substrate-induced chromophore ordering in determining the dynamical response of the system. Frey and co-workers have shown effects of the substrate on the order of ZP layers,[13] but this effect is seen in the inorganic portion of the IR spectrum (ν_a (PO_3^{2-})) rather than in the aliphatic CH_2 stretching region. We chose silicon substrates for the comparison because the surface priming chemistry is identical to that of silica, due to the 15 Å thick layer of native oxide that is present on silicon under our experimental conditions.

It is fair to consider that vibrational spectroscopy could address the question of monolayer order for ZP layers on these two substrates.[13] Aside from the different dielectric responses of the two substrates, especially in the IR spectral region, vibrational spectroscopy will not be as sensitive to order for our samples as they are for pure alkanebisphosphonate layers. Contributions from the thiophene rings combined with the structural perturbations they may induce in adjacent aliphatic domains will serve to obscure structural information for our samples. The strong absorbance of SiO_x at low energies obscures information about the inorganic portion of the structures. We therefore rely on lifetime and anisotropy measurements that are sensitive to the local environment of the oligothiophene chromophores.

The concentration dependence of the lifetime data is important in understanding excitation transport in these monolayers. If excitation transport does play a significant role in the transient response of these systems, then we would expect a highly concentration-dependent population decay.[54] The fact that we observe concentration independent lifetime behavior indicates that either excitation transport in this system does not play an important role in determining the observed motional dynamics, excitation transport dynamics are faster than can be resolved for all of the systems we examined, or the double exponential

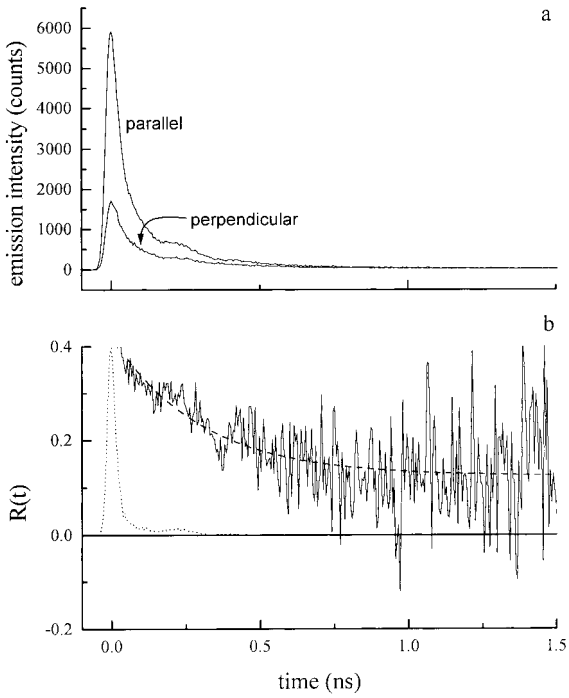

Figure 6. Emission intensities (a) and induced orientational anisotropy function (b) for a 26% BDP monolayer on silicon.

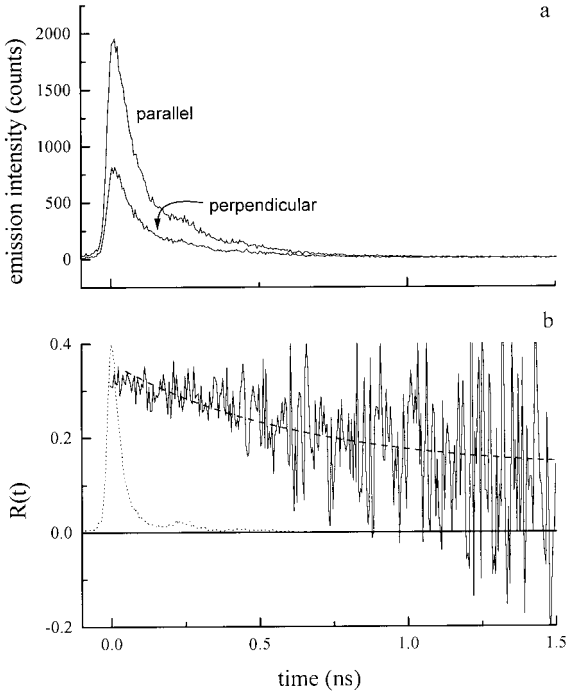

Figure 7. Emission intensities (a) and induced orientational anisotropy function (b) for a 1% QDP monolayer on silicon.

decay is itself characteristic of the excitation transport dynamics. We consider this issue in detail elsewhere.[45] The chromophores we have chosen possess moderately high fluorescence quantum yields and large absorption cross sections ($\epsilon_{max} = 27\,200$ M^{-1} cm^{-1} for BDP and 27 300 M^{-1} cm^{-1} for QDP). Because the oligothiophene chromophores relax primarily by radiative decay and they possess a large Stokes shift (Figure 1), the oligothiophene chromophores are ideal candidates for energy transport studies.[45] We are presently characterizing intralayer excitation transport in mixed monolayers of BDP and QDP. Multilayer assemblies of these chromophores will be useful in investigating interlayer excitation transport phenomena.

While the lifetime data for the chromophores reveal no discernible dependence on the identity of the substrate, the rotational dynamics of BDP and QDP on silicon are fundamentally different than those on silica. As we show in Figures 6 and 7, a measurable decay of the anisotropy is present for BDP and QDP, with an average reorientation time of ~435 ps for both, that was not seen for these chromophores bound to silica. These data were taken over a broad spectral range, with emission collected at 465 nm ± 15 nm, and the values reported in Table 2 are averaged over all concentrations because there was no statistically meaningful concentration dependence. The average tilt angles, θ, calculated from $R(\infty)$ using eq 4, are approximately the same for both QDP and BDP monolayers, ~35°, (Table 2) which correlates well with tilt angles determined for other MP monolayers.[23,55] We note that the average tilt angles of the chromophores on silica are similar, so measurement of θ cannot explain the existence of motion on the oxidized silicon substrate and not silica.

Origins of Chromophore Motion. A necessary first step is to determine the nature of the molecular motion we sense in a single layer. In particular, we need to distinguish between inter-ring isomerization and large amplitude precessional motion. The hindered rotor model describes the physics of a chromophore imbedded in a monolayer. It is typically assumed that a decay in $R(t)$ is related to large amplitude motion of a chromophore in its environment about its tether to the surface, which is one possible explanation for the dynamics we detect. If this is the dominant motion in our systems, a larger or longer chromophore would experience more hindered movement and would exhibit a correspondingly longer relaxation time. This is essentially a viscous drag argument, borrowing from the underlying principles of the Debye−Stokes−Einstein model for rotational diffusion in liquids.[56,57]

If large amplitude motion dominates our experimental data, then we would also expect to see a concentration dependence, since the thiophene chromophores occupy a larger "footprint" in the lattice sites than alkanes do. A chromophore with chromophore neighbors will move more slowly in its environment than if it were surrounded by aliphatic constituents because of geometric constraints and dipolar coupling. The average motional relaxation time, τ_{MR} (Table 2), for BDP and QDP on silicon are the same to within the experimental uncertainty, arguing that the relaxation we measure is *not* large amplitude precessional motion within a conic volume.

Another type of motion that is important in these chromophores is intramolecular relaxation, specifically the rotation of the thiophene rings about their connecting bonds. This motion is intrinsic to the molecule, and is not limited to a hindered environment.[39] As seen in Scheme 2, a transition from

(46) Horne, J. C.; Huang, Y.; Liu, G.-Y.; Blanchard, G. J. *J. Am. Chem. Soc.* Manuscript in preparation.
(47) Lipari, G.; Szabo, A. *Biophys. J.* **1980**, *30*, 489.
(48) Karpovich, D. S.; Blanchard, G. J. *Langmuir* **1996**, *12*, 5522.
(49) Smith, E. L.; Porter, M. D. *J. Phys. Chem.* **1993**, *97*, 8032.
(50) Fenter, P.; Eisenberger, P.; Li, J.; Camillone, N. III; Bernasek, S.; Scoles, G.; Ramanarayanan, T. A.; Liang, K. S. *Langmuir* **1991**, *7*, 2013.
(51) Chau, L.-K.; Porter, M. D. *Chem. Phys. Lett.* **1990**, *167*, 198.
(52) Chen, S. H.; Frank, C. W. *Langmuir* **1989**, *5*, 978.
(53) Sondag, A. H. M.; Raas, M. C. *J. Chem. Phys.* **1989**, *91*, 4926.
(54) Gochanour, C. R.; Andersen, H. C.; Fayer, M. D. *J. Chem. Phys.* **1979**, *70*, 4254.
(55) O'Brien, J. T.; Zeppenfeld, A. C.; Richmond, G. L.; Page, C. J. *Langmuir* **1994**, *10*, 4657.
(56) Debye, P. *Polar Molecules*; Chemical Catalog Co.: New York, 1929.
(57) Fleming, G. R. *Chemical Applications of Ultrafast Spectroscopy*; Academic Press: New York, 1986.

an all-anti to an all-syn conformation of QDP represents a substantial change in the orientation of the transition moments relative to the substrate. We believe that rotation of the ring(s) is more reasonable, and it can account for our data (*vide infra*). The optical anisotropy decay is a correlation function for the transition moment relaxation, so the dynamics we observe can be accounted for by inter-ring conformational changes in QDP and large amplitude motion does not need to be invoked. The anisotropy decay due to isomerization is not as pronounced for BDP as it is for QDP because BDP possesses fewer conformational degrees of freedom, but there is still a discernible change in the transition moment angle with respect to the substrate normal (Scheme 2). The BDP and QDP measured parameters of $R(0)$, τ_{MR}, and $R(\infty)$ are likely similar because they are constrained to the same molecular area, as dictated by the substrate, primer, and metal phosphonate lattice structure. Within the constraints of a well-packed, uniform monolayer, BDP and QDP may actually have the same net change in transition moment direction, because QDP will not be able to access all of the degrees of conformational freedom available to an isolated molecule (Scheme 2b).

Based on semiempirical calculations,[58−62] rotation of the thiophene rings of an isolated ground state chromophore is a low energy activated process and certainly occurs at room temperature. We have reported previously that the BDP chromophore possesses low barriers to rotation between conformations in the ground state (<1 kcal/mol).[40] This finding implies that there will be a statistical distribution of conformers that are excited, with any bias in their conformational distribution being induced by environmental, not structural constraints. In Figure 8, we show results from semiempirical calculations on QDP for twists between two end rings and between the two center rings. These plots are representative of most energetically favorable conformations, with the exclusion of contributions from the twist between the other two end rings, which were held at 0° in the anti conformation. In the first excited singlet state, energetic minima are present at approximately 0° and 180° ring torsion (anti and syn), while a maximum of ∼10 kcal/mol is calculated for an inter-ring angle of 90°. This maximum is the result of the tendency of thiophenes to form a planar quinoid structure in the excited state. The syn and anti conformations correspond to the lowest energy difference between S_0 and S_1, so transitions associated with these conformations are expected to produce the red shifted features we see. From these calculations we can see that QDP exhibits facile interconversion between all conformations in the ground state and the excited-state possesses definite minima. These calculations are, of course, qualitative and are limited by the utility of the PM3 parametrization in the calculation of S_1 surfaces. Despite these limitations, they do demonstrate the likelihood for the chromophores to exhibit ring rotation in the S_1, consistent with intramolecular relaxation being the dominant phenomenon we detect in the dynamical measurements.

The semiempirical calculations serve to limit the possible explanations for why we observe motional relaxation for monolayers on oxidized Si(100) and not on fused silica. The observation of motion on the silicon substrate could be taken to imply that we are observing motion in this system because the rotation of the chromophore rings is not hindered. It is clear

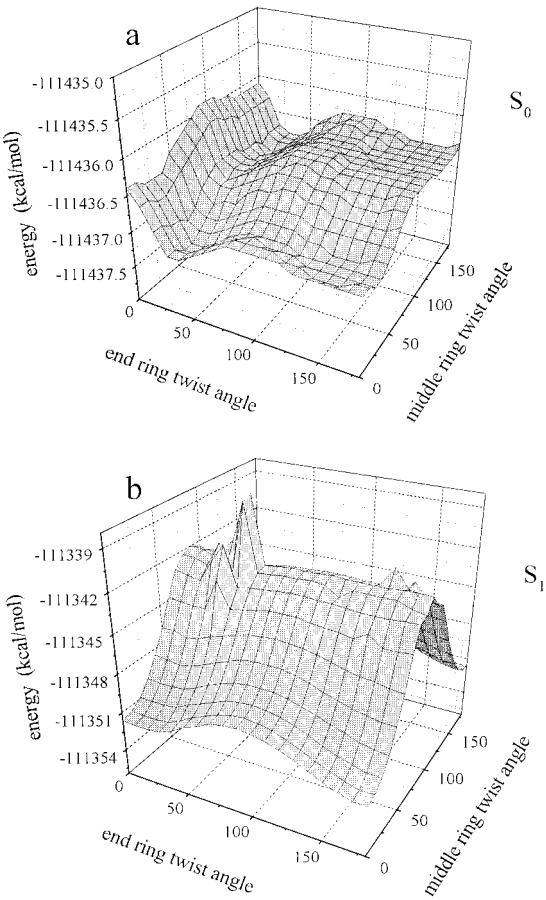

Figure 8. Calculated energy barriers for QDP inter-ring rotation for the first two inter-ring bonds: (a) S_0 and (b) S_1. Twist angles indicated are for angles with respect to their adjacent ring.

based on the data for the Si(100) substrate and comparison to bulk liquid data that motion of the thiophene rings on silica would occur within a time window accessible to our measurements. We believe that thiophene ring rotation on the silica substrate must be hindered in some way. A simple difference in the dielectric responses of the two substrates cannot account for the differences in motional behavior, because the population dynamics, which depend sensitively on the dielectric response of the substrate, do not vary.

The surface morphology of the substrates is more likely to provide an explanation for our observations. As shown in atomic force microscopy (AFM) images (Figure 9), the two substrates are characterized by very different surface features. The silica has a granular, irregular surface, and the oxidized silicon exhibits striations, probably a result of polishing. The grooves in the oxidized Si surface are 200−500 Å apart and 10−30 Å deep. The roughness of the two surfaces was determined from the fwhm of a histogram of the imaged area, which is slightly narrower for the silica substrate. On a length scale more relevant to our spectroscopic measurements (50 Å),[63] the variations in height across the surfaces reveal much flatter domains on silica (±2 Å) than on silicon (±10 Å). Because of the greater variation in surface relief, chromophores on silicon should have more motional freedom than on a corresponding monolayer formed on silica. An additional piece of information

(58) Dewar, M. J. S.; Zoebisch, E. G.; Healy, E. F.; Stewart, J. J. P. *J. Am. Chem. Soc.* **1985**, *107*, 3902.
(59) Dewar, M. J. S.; Dieter, K. M. *J. Am. Chem. Soc.* **1986**, *108*, 8075.
(60) Stewart, J. J. P. *Comput.-Aided Mol. Des.* **1990**, *4*, 1.
(61) Dewar, M. J. S.; Thiel, W. *J. Am. Chem. Soc.* **1977**, *99*, 4899.
(62) Dewar, M. J. S.; Thiel, W. *J. Am. Chem. Soc.* **1977**, *99*, 4907.

(63) We estimate the Förster critical transfer radius for these chromophores to be 25 Å. For rotational diffusion measurements, the relevant distance is probably shorter, on the order of the nearest neighbor spacing. Due to the amorphous nature of these surfaces, we can only estimate this distance to be ≤ 10 Å.

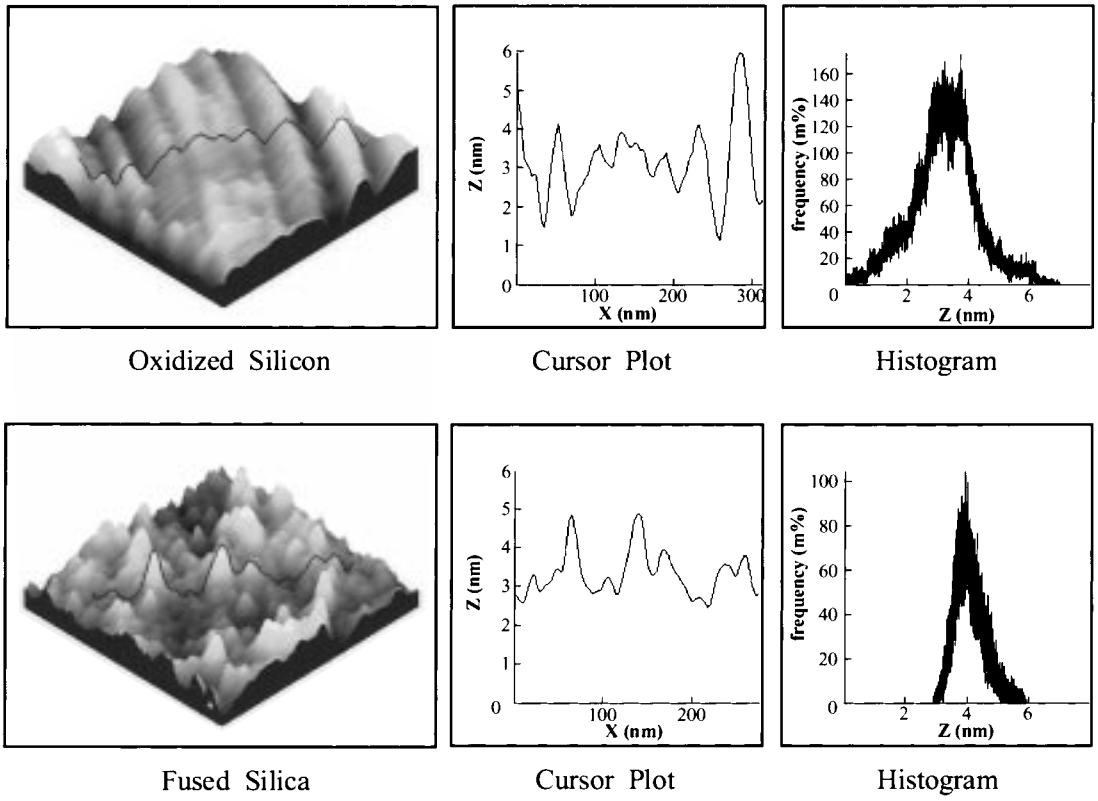

Figure 9. Atomic force microscopy images for 300 nm × 300 nm areas of oxidized silicon (top) and fused silica (bottom) substrates. Cursor plots show height profiles along the line indicated in the 3-D images. Image histograms indicate surface relief (Δz) distribution of area imaged.

that corroborates this explanation is that for SiO_x, $x_{silicon} < x_{silica}$, which could result in a less dense layer on silicon. Haller has shown that, for this priming chemistry on silicon, under all except the most stringent conditions, the triethoxysilane primer polymerizes easily, resulting in large islands on the surface instead of a single layer.[64] It is possible that the higher density of hydroxyl active sites on the silica surface precludes much of the polymerization because the tighter packing does not allow as much multilayer buildup. For silicon, with fewer active sites on which to grow the bisphosphonate monolayer, the chromophores will be spaced further apart, and therefore ring rotation is less hindered. The relative active site density for the two substrates does not explain, however, why we observe a larger fluorescence signal from the monolayers on silicon than on silica. One factor is that the polished silicon substrate is more reflective, so that a larger fraction of emitted light is collected. A more important factor is that, in the more dense monolayers on silica, aggregation of the chromophores is likely. Aggregates typically exhibit lower emission quantum yields than isolated chromophores,[65] and the less densely packed monolayers on silicon will, on average, have more nonaggregated chromophores. Regardless of these qualitative observations relating to emission intensity, our motional relaxation data can be understood in the context of substrate roughness, as characterized by the AFM data.

Conclusion

The lifetime and motional dynamics of oligothiophene chromophores within ZP monolayers reveal a subtle difference in the monolayers formed on different substrates. For both silica and oxidized Si(100) substrates, the fluorescence lifetime behavior of each chromophore is identical and is concentration independent, pointing to the limited contribution of intralayer excitation transport in these systems. Transient anisotropy measurements reveal that, for both substrates, the chromophores are oriented at ~35° with respect to the surface normal. For monolayers formed on silica, there is no evidence for chromophore motion, while motion is seen for monolayers formed on the silicon substrate. Despite the substantial similarity between the two families of monolayers, the surface roughness of the polished silicon substrate allows for greater motional freedom of the chromophores in the monolayers. The comparatively lower site density for active hydroxyl groups on the oxidized Si(100) surface likely also plays a role in determining the observed dynamics. These data underscore the important role of substrate morphology in determining the properties of molecular interfaces and provide a foundation for the examination of interlayer excitation transport studies.

Acknowledgment. We are grateful to the National Science Foundation for support of this work through Grant CHE 95-08763. We are deeply indebted to Prof. G. Y. Liu and Y. Huang (Wayne State University) for their assistance in AFM imaging of the oxidized silicon and fused silica substrates.

JA972574I

(64) Haller, I. *J. Am. Chem. Soc.* **1978**, *100*, 8050.

(65) Song, Q.; Bohn, P. W.; Blanchard, G. J. *J. Phys. Chem. B.* **1997**, *101*, 8865.